ECOLOGY LETTERS

Ecology Letters, (2011) doi: 10.1111/j.1461-0248.2011.01598.x

LETTER

Changes in forest productivity across Alaska consistent with biome shift

Pieter S. A. Beck,[1]* Glenn P. Juday,[2] Claire Alix,[3] Valerie A. Barber,[2] Stephen E. Winslow,[2] Emily E. Sousa,[2] Patricia Heiser,[2] James D. Herriges[4] and Scott J. Goetz[1]

Abstract

Global vegetation models predict that boreal forests are particularly sensitive to a biome shift during the 21st century. This shift would manifest itself first at the biome's margins, with evergreen forest expanding into current tundra while being replaced by grasslands or temperate forest at the biome's southern edge. We evaluated changes in forest productivity since 1982 across boreal Alaska by linking satellite estimates of primary productivity and a large tree-ring data set. Trends in both records show consistent growth increases at the boreal–tundra ecotones that contrast with drought-induced productivity declines throughout interior Alaska. These patterns support the hypothesized effects of an initiating biome shift. Ultimately, tree dispersal rates, habitat availability and the rate of future climate change, and how it changes disturbance regimes, are expected to determine where the boreal biome will undergo a gradual geographic range shift, and where a more rapid decline.

Keywords

Boreal forests, drought, evergreen forests, global warming, high latitudes, NDVI, productivity, remote sensing, tree rings.

Ecology Letters (2011)

INTRODUCTION

Over the 21st century, dynamic global vegetation models predict that the boreal biome is likely to experience forest conversion and losses resulting in a northward shift in the biome's range, particularly under scenarios of greatest warming (Lucht *et al.* 2006; Scholze *et al.* 2006; Gonzalez *et al.* 2010). As northern high latitude forest ecosystems contain at least 30% of global terrestrial carbon (McGuire *et al.* 2009; Tarnocai *et al.* 2009), such changes could substantially modify future climate (Bonan 2008). Northward and elevational shifts in species distributions over the past decades have been documented across a wide range of taxa (Hickling *et al.* 2006). At high latitudes shrub abundance has increased (Tape *et al.* 2006) and in alpine environments forest communities have recently migrated to higher elevations, apparently in response to environmental warming (Peñuelas & Boada 2003). At regional scales, however, there is little evidence of directional change in the distribution of terrestrial biomes attributable to ongoing climate change.

Model simulations of high latitude ecosystems changes in the last three decades, which experienced rising atmospheric CO_2 concentrations and associated warming (Rahmstorf *et al.* 2007), suggest an increasing vegetation productivity trend (Lucht *et al.* 2002; Kimball *et al.* 2007; Zhao & Running 2010). Analyses of satellite imagery since 1982 have generally supported this view, indicating consistent increases in gross primary productivity estimated using remote sensing (Prs; Myneni *et al.* 1997; Zhou *et al.* 2001). Recent field measured increases in tundra shrub growth over the same period are also in agreement with model outputs (Forbes *et al.* 2010). Populations of far northern trees in cold marginal environments have sustained positive growth responses to temperature, and in recent decades have grown at their greatest recorded rates (Juday *et al.* 2005). In contrast, spatially restricted field observations have documented anomalously low white spruce (WS) [*Picea glauca* (Moench) Voss] growth in productive stands in interior Alaska in the last three decades of the 20th century (Barber *et al.* 2000). Similar observations at elevational tree line in Canada indicate that once the climate warms beyond a physiological threshold, a divergence of tree growth and air temperature occurs (D'Arrigo *et al.* 2004). A few satellite-based studies report a recent reversal of the initial (1982 through 1991) productivity gains of boreal forest across many high latitude forest areas (Angert *et al.* 2005; Goetz *et al.* 2005), but these observations have not been directly linked to field measurements.

Tree-ring measurements provide a consistent record of past productivity but are traditionally collected at ecosystem transition zones (ecotones) to test for climate sensitivity or to reconstruct climate records (D'Arrigo *et al.* 2004), rather than to capture growth trends in more typical (higher density) forest stands. As a result, comparisons of *in situ* tree growth measurements with more synoptic scale observations across large spatial domains, such as satellite data, are rare (Kaufmann *et al.* 2004). Establishing this link provides a potentially powerful way to extend relatively limited field observations to the spatial domain covered by remote sensing observations, and thus provide a comprehensive view of biome-wide productivity patterns and trends.

[1]*Woods Hole Research Center, Falmouth, MA 02540, USA*
[2]*School of Natural Resources and Agricultural Sciences, University of Alaska Fairbanks, Fairbanks, AK 99775, USA*
[3]*Archéologie des Amériques, NRS/Université de Paris 1 – Panthéon Sorbonne, France*
[4]*Bureau of Land Management, Fairbanks, AK 99709, USA*
**Correspondence: E-mail: pbeck@whrc.org*

Spruce species dominate the boreal forest biome of North America. We collected an extensive tree-ring width data set from WS and, for the first time, from black spruce [BS, *Picea mariana* (Mill.) B.S.P.] forest stands which, despite their dominance in boreal North America, have rarely been reported in the dendrochronology literature. The WS and BS stands span an east–west gradient from a drier continental to a more mesic maritime climate, and were sampled to capture variations in forest productivity. We compared this data set to satellite remote sensing observations of the normalized difference vegetation index (NDVI), a spectral metric reflecting gross productivity (Prs; Myneni *et al.* 1995; Goetz & Prince 1999). Spatial coherence and temporal covariance of these two very different observational records was assessed along with their interannual variability, to evaluate geographical patterns in changes in vegetation productivity over the period of their coincidence (1982–2008). Here, we investigate these patterns to test the hypothesis that the boreal biome is undergoing a range shift characterized by: (1) productivity increases at the boreal–tundra ecotone and (2) productivity declines at the warmer margin of its current distribution.

MATERIAL AND METHODS

Remotely sensed gross productivity (Prs) 1982–2008

Remotely sensed gross productivity was mapped annually from a gridded time series as the mean NDVI during the growing season, while accounting for spatial variation in the growing season length (GSL). The NASA Global Inventory Modeling and Mapping Studies data set (GIMMS-NDVI version G) spans the period 1982–2008 (http://glcf.umiacs.umd.edu/data/gimms/; Tucker *et al.* 2005) at 0.07° spatial resolution. It was derived from measurements by the Advanced Very High Resolution Radiometers (AVHRRs) carried by the afternoon-viewing NOAA satellite series (NOAA 7, 9, 11, 14, 16 and 17). The data processing includes corrections for atmospheric aerosols effects from the El Chichón and Pinatubo eruptions, solar zenith angle effects and sensor differences and degradation (Tucker *et al.* 2005). GIMMS-NDVI provides 24 global NDVI images per year, with the first image of each month representing the month's first 15 days, and the other image the remainder.

We mapped Prs for each year between 1982 and 2008. First, the GSL was mapped at 30 arc-second (0.0083°) spatial resolution from the Moderate Resolution Imaging Spectroradiometer (MODIS) Land Cover Dynamics product (MOD12Q2; Zhang *et al.* 2006). Here, the GSL was initially estimated as the period between the latest 'start of greening' date, and the earliest 'start of dormancy' date recorded in the MOD12Q2 data between 2001 and 2004. To ensure exceptionally late snow melt or early snow fall events never overlapped with our growing season estimate, the initial GSL estimate was shortened by a third. The resulting maps of GSL were then averaged to the spatial and temporal resolution of the GIMMS-NDVI data to determine the GSL for each GIMMS-NDVI grid cell (see Figure S1). Next, Prs was calculated and mapped annually from GIMMS-NDVI as the mean NDVI during the growing season, using the GSL map to account for spatial variation in the GSL. To account for year-to-year variation in the start and end of the growing season, each year Prs was set to the maximum value output from a time series moving average, with window length set to GSL (Figure S2).

To map trends in Prs, the NDVI data were further filtered to mask anthropogenic changes and non-deterministic (e.g. stochastic) series. The MODIS Land Cover map for 2005 (MOD12Q1; Friedl *et al.* 2002), with a spatial resolution of 15 arc-seconds (0.0042°), was reclassified from the International Geosphere-Biosphere Programme (IGBP) classification to (1) anthropogenic land cover, be it agricultural (IGBP-12, IGBP-14), or urban (IGBP-13), (2) non-vegetated (IGBP-0, IGBP-15, IGBP-16) or (3) vegetated (other IGBP classes). A GIMMS grid cell was excluded from the analysis if more than 40% of it was classified as non-vegetated or if vegetated land cover was not at least three times larger than anthropogenic land cover.

Patterns in Prs changes were compared with gradients of (1) tree cover as mapped in the MODIS Vegetation Continuous Fields product (MOD44; Hansen *et al.* 2003) and (2) monthly temperatures in the 1982–2008 period (McKenney *et al.* 2006). Both were gridded to match the GIMMS data set.

Burn history

In each GIMMS grid cell in Alaska and Canada, the yearly area burned was calculated from 1950 to 2007 by merging the fire perimeter data produced by the Bureau of Land Management, Alaska Fire Service (AFS; acquired from the Alaska Geospatial Data Clearinghouse, http://agdc.usgs.gov/data/blm/fire), and the Fire Research Group at the Canadian Forest Service.

Tree-ring sampling

We measured radial growth in 839 mature trees, of which 627 WS and 212 BS, that were dominant in the current landscape and had no visible signs of fire or insect damage. The trees were pooled to create 46 WS and 42 BS stand-level wood growth (WG) estimates, based on the GIMMS grid cell the trees were located in. The number of trees sampled in a stand varied from 1 to 62, with a median of 6. Mean stand-level growth was calculated from 1982 until the year of sampling, generating 88 series between 6 and 27 years long (median = 20) where growth and GIMMS data could be paired.

Tree-ring data were not de-trended as spruce trees of the age range in this study exhibit little to no age-related growth trend (Barber *et al.* 2000). Furthermore, Barber *et al.* (2000) showed for a subset of the current data set that de-trending had negligible effects on the growth–climate relationships. Mean radial growth was calculated per stand from non-normalized tree-ring series to preserve the greater contribution of larger trees to stand-level WG. An index of topography-related soil wetness was estimated for the tree stands from a 60-m digital elevation model, and calculated as $\ln(\alpha/\tan\beta)$ where α is the local upslope area draining through a certain point per unit contour length and $\tan\beta$ is the local slope (Beven & Kirkby 1979).

Statistical methods

Prior to mapping, temporal trends in Prs were subjected to a Vogelsang test (Vogelsang 1998) to determine if a deterministic temporal trend was present in the data (statistical significance was set at $\alpha = 0.05$). The Vogelsang stationarity test controls for the possibility of strong serial correlation in the data generating spurious trends. It is valid whether errors are stationary or have a unit root, and does not require estimates of serial correlation nuisance parameters. It is useful for masking stochastic changes in Prs in the landscape such as those associated with disturbance (Goetz *et al.* 2005).

The consistency of temporal changes in both tree growth series and Prs since 1982 was quantified and compared using Kendall's τ (Hollander & Wolfe 1973), calculated at each site from the cross-tabulation of time and radial growth (τ_{growth}), and time and Prs (τ_{Prs}). As a result, τ approaches 1 as a series consistently increases with time, and −1 as it consistently decreases with time. Agreement between trends in Prs and growth was quantified using a regression model describing τ_{growth} as a linear function of τ_{Prs}, weighted by the number of available ring width measurements. The regression included both BS and WS sites, but excluded sites with evidence of burning since 1950.

To compare year-to-year variation in Prs and growth in isolation from multi-year trends, the agreement between yearly changes in radial growth (Δgrowth) and Prs (ΔPrs) was calculated at each site using Kendall's τ, denoted as $\tau_{\Delta Prs,\Delta growth}$. Agreement was calculated separately in years of increasing growth (Δgrowth > 0), and decreasing growth (Δgrowth < 0), and only if 5 years of observations were available. The agreement was then assessed for statistical significance across sites using the Wilcoxon signed rank test (H_0: $\tau_{\Delta Prs,\Delta growth} = 0$).

RESULTS

Over the satellite record, which begins in 1982, within-stand variation in tree growth trends was present: 48 of 88 stands contained both trees displaying positive ($\tau_{ring\ width} > 0$) and negative growth trends ($\tau_{ring\ width} < 0$). However, mean interseries correlation of raw ring widths during the reference growth period of 1950 to date of collection was generally high [for stands with 10 trees or more, mean = 0.43 (±0.14 SD), $N = 31$] indicating that our tree-ring based estimates of stand-level WG are robust, particularly in the larger samples.

Across boreal Alaska both WG and satellite-derived Prs predominantly declined since 1982, except in the more maritime areas of the West (Fig. 1). Across tree-ring sites where the remote sensing data indicated non-stochastic trends in gross productivity ($N = 30$, Vogelsang test, $\alpha = 0.05$; see Table S1), yearly values of WG and Prs were strongly positively correlated and displayed a negative temporal trend between 1982 and 2008 ($R = 0.69$, $N = 27$ years, $P < 0.001$; Fig. 2). Furthermore, all but 2 of these 30 sites (13 WS and 17 BS), showed an identical direction of change in WG and Prs as measured by the signs of τ_{growth} and τ_{Prs} respectively. Across all sites without traces of fire since 1950, temporal changes in Prs since 1982 reflect commensurate changes in spruce growth [Fig. 3; $\tau_{growth} = \tau_{Prs} * 1.06(\pm 0.14\ SEM) - 0.001(\pm 0.05\ SEM)$, d.f. = 55]. Overall, the best agreement in trends occurred when growth was estimated from a larger number of samples (Figure S3).

Decreases in WG relative to the previous year were weakly correlated with changes in Prs (median $\tau_{\Delta Prs,\Delta growth} = 0.2$, $P = 0.002$, $N = 21$). By contrast, increases in WG from 1 year to the next were not consistently associated with equivalent increases in Prs (median $\tau_{\Delta Prs,\Delta growth} = -0.05$, $P = 0.59$, $N = 21$), suggesting that resource allocation to leaf mass and WG is not necessarily regulated at identical time scales.

While the tree-rings used here were collected from mature trees in unburned stands, the satellite Prs time series reflects the legacy of wildfire. The magnitude of that effect is dependent upon the timing, extent and severity of burning (Goetz *et al.* 2006). Consequently, trends in WG and Prs may not agree in some areas characterized by vegetation mortality from fire (sudden decrease in Prs) or rapid vegetation regrowth following fire (steady increase in Prs; Figure S4). After excluding disturbance-related stochastic changes in Prs using the burn history data and the Vogelsang test (Goetz *et al.* 2005), the tundra areas of Alaska show near-ubiquitous increases in Prs (Fig. 1). The coldest boreal areas, which are currently sparsely forested, i.e. those at the boreal–tundra ecotone, also display deterministic increases in productivity over the past three decades (Fig. 4).

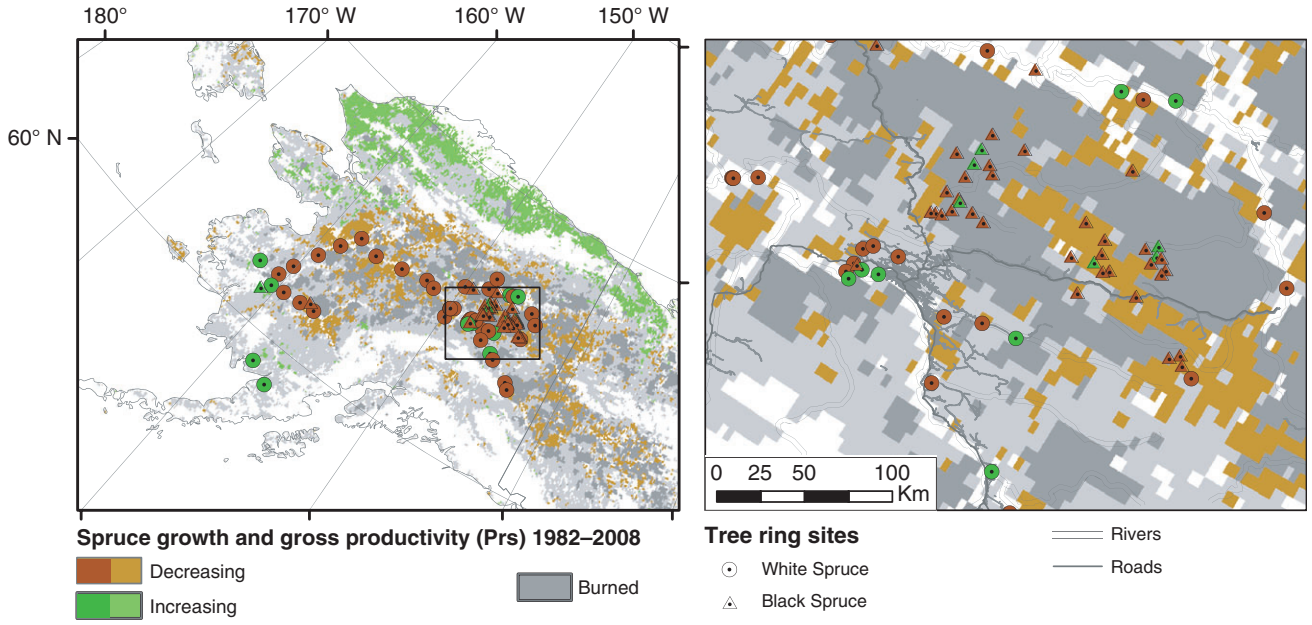

Figure 1 Trends in remotely sensed gross productivity (Prs) between 1982 and 2008 and trends in spruce growth since 1982 in Alaska (left) and the area around Fairbanks (right). White shading indicates sparsely vegetated or human modified land cover. Light grey shading indicates the trend in Prs from 1982 to 2008 was non-deterministic based on a Vogelsang significance test ($\alpha = 0.05$), and dark grey areas had wildfires anywhere between 1982 and 2007. Green and brown shading in the symbols indicate increasing and decreasing ring widths, respectively, in unburned stands from 1982 to the year of sampling which ranged from 1994 to 2008.

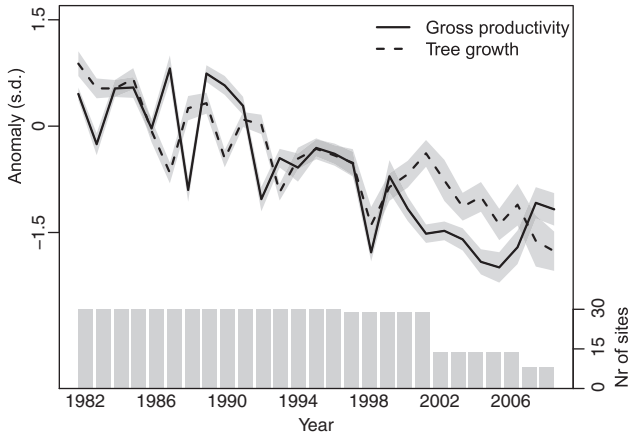

Figure 2 Trends in remotely sensed gross productivity (Prs, solid line) and radial tree growth (dashed line) at the 30 tree-ring sampling sites with deterministic changes in Prs based on a Vogelsang test ($\alpha = 0.05$; Vogelsang 1998). Anomalies are expressed in units of standard deviations (SD) from the respective means calculated over the period 1982–1996. Lines represent yearly mean anomalies across all sites and shaded areas their standard errors, both weighted by the number of trees sampled at each site.

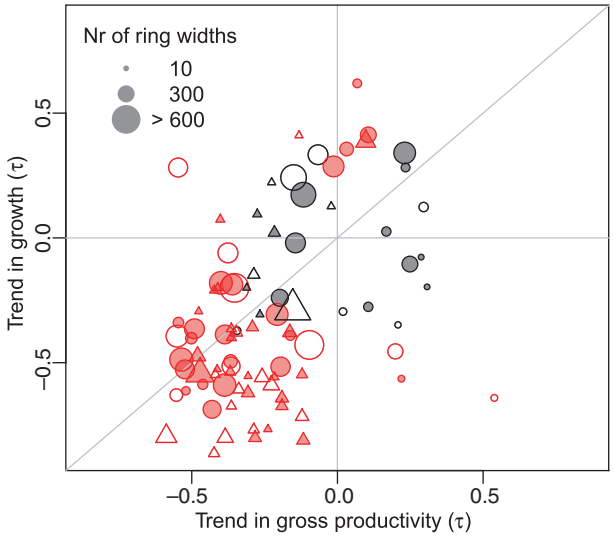

Figure 3 Temporal trends in WG and Prs. Growth is calculated from ring widths of all trees sampled within a single satellite grid cell (*c.* 64 km^2), and point sizes are equivalent to the number of ring widths in the series, which were restricted to years when both Prs and growth data were available. Circles represent white spruce stands and triangles black spruce stands. Open symbols indicate vegetation burning and regrowth after 1950 might have influenced Prs estimates. Red points represent cases where τ of the Prs series or the WG series were statistically different from 0 ($\alpha = 0.05$).

In contrast, all other forested areas in the boreal zone, not only the warmest or most densely forested ones, were dominated by productivity declines (Figs 1 and 4). Topographical wetness (W) did not differ significantly between sites where productivity increased or decreased, whether measured as WG or satellite-derived gross productivity (Kruskall–Wallis rank sum test, H_0: $W_{\tau WG<0} = W_{\tau WG>0}$, $P = 0.3$; H_0: $W_{\tau Prs<0} = W_{\tau Prs>0}$, $P = 0.1$; $N = 88$) and at 8 of the 10 wettest sites both measures indicated declining productivity.

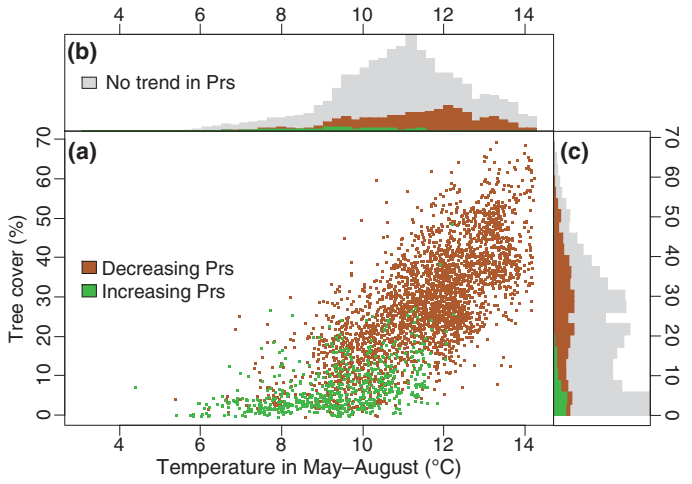

Figure 4 (a) Tree cover (Hansen *et al.* 2003) compared to mean air temperature in May–August in 1982–2007 for non-anthropogenic vegetated areas of interior Alaska, i.e. the mainland north of the Alaska Range and south of the Brooks Range. Only areas where gross productivity (Prs) shows a deterministic trend from 1982 to 2008 and where there were no wildfires between 1982 and 2007 are shown. Histograms represent the distribution of (b) temperature and (c) tree cover and include areas where no trend was detected.

DISCUSSION

Along with temperature, tropospheric ozone, nitrogen deposition and CO_2 concentrations have all increased globally in the last three decades, potentially driving shifts in vegetation productivity (IPCC 2007). Mean ozone concentrations in Alaska are low compared to more populated areas, and are generally considered to be at global 'background levels' (Figure S5; Vingarzan 2004). Because of this and the greater tolerance of needle-leaved trees to elevated ozone concentrations (Sitch *et al.* 2007; Wittig *et al.* 2009) projected increases in ozone over the 21st century are not expected to adversely affect vegetation productivity in Alaska (Sitch *et al.* 2007), and recent increases are unlikely to explain the patterns in productivity documented here. Similarly, the relatively low rates of nitrogen deposition in interior Alaska [at Denali National Park; Jones *et al.* (2005) report 0.3 kg N ha^{-1} year^{-1}] are an order of magnitude lower than rates that were experimentally found to limit boreal tree growth (Hogberg *et al.* 2006). This is consistent with recent results from a process-based biogeochemistry model with coupled carbon and nitrogen cycles that indicates that over the past five decades N deposition has had a very small effect on boreal net ecosystem exchange (McGuire *et al.* 2010). These same model simulations indicate that increased atmospheric CO_2 concentrations since 1750 have promoted net uptake of carbon by arctic as well as boreal ecosystems, i.e. a CO_2 fertilization effect. At the pan-arctic scale, however, this effect appears outweighed by a stronger increase of carbon losses from the biosphere to the atmosphere due to shifts in fire disturbance and climate (mediated by combustion and temperature, moisture, and successional controls on photosynthesis and respiration), to the extent that the CO_2 fertilization is not likely to be detectable over the 30-year period investigated here (McGuire *et al.* 2010). Overall, we conclude that the productivity patterns we document in mature unburned forests are driven more by climate (temperature and moisture) than ozone, nitrogen or CO_2 fertilization effects.

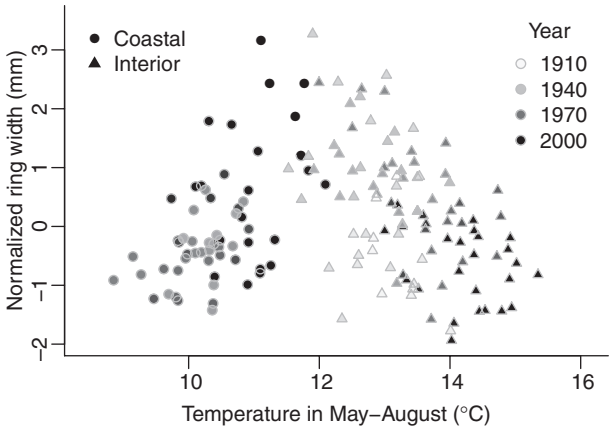

Figure 5 Normalized white spruce mean tree-ring widths at coastal and interior sites where trees were sampled in 2010 vs. mean temperature in May–August of the year of ring growth and 1 and 2 years prior. The coastal trees were sampled at Dillingham (N = 10) and King Salmon (N = 8; Table S1) and compared with the temperature record at King Salmon Airport (59° N, 157° W) which starts in 1947. The trees from interior Alaska were sampled in the Yukon River Flats (N = 25; Table S1) and were compared with the Fairbanks/University Experiment Station (65° N, 148° W) temperature record which is the longest one available in interior Alaska and representative of interannual variation across the region (Barber *et al.* 2000). We note that the choice for the months of May–August as a temperature index represents a compromise since seasonal temperature sensitivity differs between the sites (Figure S6).

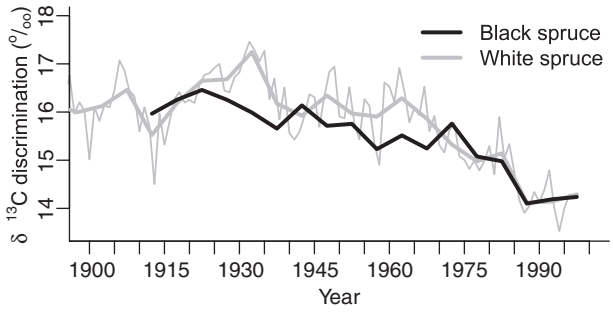

Figure 6 Stable carbon isotope ($\delta^{13}C$) time series for black spruce and white spruce stands in interior Alaska. Black spruce data were measured in the Zasada Road 8 stand at the Bonanza Creek Long-term Ecological Research (LTER) site (64.8° N, 148.0° W) following the methods described by Barber *et al.* (2000) and at 5-yearly intervals to assure sufficient wood material was available for analysis. Yearly white spruce $\delta^{13}C$ discrimination (thin grey line) was taken from Barber *et al.* (2000), measured in the Reserve West stand in the same LTER site and averaged at 5-year intervals (bold line). Isotopic discrimination is expressed as the proportional deviation of the measured $^{13}C/^{12}C$ ratio from the Peedee belemnite carbonate standard (Craig 1957).

The observed spatiotemporal pattern in productivity suggests that in colder areas temperature limitations on spruce growth have been released during the recent decades of warming, while the climate has shifted beyond the optimum for spruce growth in the warmer zones of interior Alaska (Figs 4 and 5). Earlier analysis of carbon isotopes in WS has attributed the growth declines in interior Alaska to temperature-induced drought stress (Barber *et al.* 2000). Additional analysis of BS tissue reveals an equally strong drought-induced shift in isotopic composition since the early 1980s (Fig. 6, Appendix S1), suggesting that water availability is increasingly limiting productivity of the dominant tree species in Alaskan boreal forests.

Drought in boreal forests can originate from a lack of soil moisture or an excessive evaporative demand. Although summer precipitation has been experimentally shown to limit productivity of spruce trees (Yarie 2008), it does not show a directional change in Alaska during the decades investigated here (Hinzman *et al.* 2005). Our finding that recent decreases in productivity are not restricted to upland sites, but are equally prominent in floodplains where ground water could buffer against precipitation-driven water deficits (Viereck *et al.* 1993), further indicates that soil moisture is not the main driver of the widespread declines in productivity. In contrast to soil moisture stress, evaporative demand has grown during the last decades; even during periods when temperatures were relatively stable (Figure S7). This supports our contention that observed decreases in productivity are the result of drought stress stemming from hydraulic limitations imposed by high vapour pressure deficits (VPDs) on photosynthesis during warm summer periods. Furthermore, because plant growth responds nonlinearly to both VPD and temperature, which are coupled, this observation is consistent with the temperature–growth relationship reported here (Fig. 5).

Negative productivity trends in the Alaskan boreal forest are particularly pronounced since the mid-1990s (Fig. 2), in contrast to widespread productivity increases in both forest and tundra areas in the preceding decade (Figure S8a; Myneni *et al.* 1997). Since the mid-1990s, we observe a divergent response to climate warming in Arctic tundra and forests, consistent with earlier reported NDVI trends across North America (Goetz *et al.* 2005) and Alaska (Verbyla 2008). Whereas the warmer climate has continued to increase tundra productivity, it appears to constrain photosynthetic activity in boreal forests (Fig. 1; Figure S8a). Recent global ecosystem model simulations showing increased net primary productivity in both forested and tundra areas in Alaska from 2000 to 2009 (Zhao & Running 2010) apparently fail to capture the declines we observe using satellite imagery (Figure S8b). As plant respiration generally increases with temperature, increased net productivity is at odds with the gross productivity declines we observed in undisturbed mature boreal forest. While net productivity increases are consistent with assumed metabolic responses to rising temperature in cold climates, the recent simulation results currently show no moisture limitations on Alaskan vegetation productivity (Zhao & Running 2010). In contrast, our observations indicate that the higher temperatures of recent decades have limited productivity of Alaskan forests owing to coincident increases in evaporative demand (VPD; Figure S7), which is consistent with experimental and *in situ* measurements (Barber *et al.* 2000; Hogg *et al.* 2008; Way & Oren 2010), as well as earlier model simulations (e.g. Angert *et al.* 2005; Zhang *et al.* 2008).

The observed changes in forest productivity during the period of the satellite record (27 years), and their relationship to temperature, indicate that warming has resulted in drought stress exerting an increasingly limiting role on both Prs and tree growth across most of the boreal forest ecosystem of interior Alaska. We observed increasing tree growth and Prs only in the marginal zone of low tree cover in western Alaska, which constitutes the boreal–tundra ecotone, and beyond current tree limits, both areas where 20th century temperatures were sub-optimal for tree growth. An identical pattern of shifts in boreal forest productivity has been projected by global vegetation models to occur over the course of the 21st century, leading to biome-wide changes such as northward forest expansion and regional drought-induced forest recession (Lucht *et al.* 2006; Scholze *et al.* 2006). The confluence of the current observational record with the

latter longer term projections thus provides support for the hypothesis that a biome shift is already underway on a quasi-continental scale. As long as increases in temperature persist, currently forested areas will experience intensified stress, mortality and composition changes, while the transitional ecotones of western and northern Alaska will become climatically more suitable for enhanced tree recruitment and growth associated with forest migration.

Ultimately, the resiliency of the boreal forest to climate change and the possibility for forest migration, as dictated by tree dispersal rates and habitat availability, will shape the extent and speed of a biome shift. Both the *in situ* tree ring and the satellite data presented here suggest that the climate of the last few decades has shifted beyond the physiological optimum for spruce growth throughout the Alaskan boreal ecosystem. Intensified monitoring is needed to document whether the pattern observed here will result in a rapid decline of the boreal biome rather than a more gradual geographical range shift, particularly since direct effects of climate warming on tree growth can amplify its indirect effects, e.g. through increased susceptibility to insect disturbance (Malmström & Raffa 2000). Moreover, forest expansion into tundra areas is expected to vary geographically, since it too is impacted by indirect climate effects, such as thermokarst and fire, and can be physiologically limited by drought (Lloyd *et al.* 2002; D'Arrigo *et al.* 2004). Finally, if the continued shift in the climate optimum for forest growth outpaces tree migration rates, a contraction of the boreal biome in the 21st century is more likely than a northward or elevational shift in its distribution.

ACKNOWLEDGEMENTS

We thank John Little of the Canadian Forest Service for providing the Canadian fire database, Dave McGuire for his responses to queries on biogeochemical cycles in Alaska and the anonymous referees for their constructive comments. We acknowledge support from the National Science Foundation (0902056), the NOAA Carbon Cycle Science program (NA08OAR4310526) and the NASA Carbon program (NNX08AG13G) to SJG, from the McIntire-Stennis Cooperative Forestry Research Program, the US Geological Survey Yukon River Basin program, and the US NSF Long-Term Ecological Research (LTER) Program (DEB 0620579) to GPJ, and from the French Polar Institute Paul Emile Victor (IPEV) programme 402 Anthropobois, the International Arctic Research Center (G1464, NSF ARC-0327664 and G191, NOAA NA17RJ1224), the NSF Office of Polar Programs (0436527) and the Geist Fund of the University of Alaska Museum of the North to CA.

REFERENCES

Angert, A., Biraud, S., Bonfils, C., Henning, C.C., Buermann, W., Pinzon, J. *et al.* (2005). Drier summers cancel out the CO_2 uptake enhancement induced by warmer springs. *Proc. Natl. Acad. Sci. USA*, 102, 10823–10827.

Barber, V.A., Juday, G.P. & Finney, B.P. (2000). Reduced growth of Alaskan white spruce in the twentieth century from temperature-induced drought stress. *Nature*, 406, 668–673.

Beven, K.J. & Kirkby, M.J. (1979). A physically based, variable contributing area model of basin hydrology. *Hydrol. Sci. Bull.*, 24, 43–69.

Bonan, G.B. (2008). Forests and climate change: forcings, feedbacks, and the climate benefits of forests. *Science*, 320, 1444–1449.

Craig, H. (1957). Isotopic standards for carbon and oxygen and correction factors for mass spectrometric analysis of carbon dioxide. *Geochim. Cosmochim. Acta*, 12, 133–149.

D'Arrigo, R.D., Kaufmann, R.K., Davi, N., Jacoby, G.C., Laskowski, C., Myneni, R.B. *et al.* (2004). Thresholds for warming-induced growth decline at elevational tree line in the Yukon Territory, Canada. *Global Biogeochem. Cycles*, 18, GB3021.

Forbes, B.C., Fauria, M.M. & Zetterberg, P. (2010). Russian Arctic warming and 'greening' are closely tracked by tundra shrub willows. *Glob. Change Biol.*, 16, 1542–1554.

Friedl, M.A., McIver, D.K., Hodges, J.C.F., Zhang, X.Y., Muchoney, D., Strahler, A.H. *et al.* (2002). Global land cover mapping from MODIS: algorithms and early results. *Remote Sens. Environ.*, 83, 287–302.

Goetz, S.J. & Prince, S.D. (1999). Modeling terrestrial carbon exchange and storage: evidence and implications of functional convergence in light use efficiency. *Adv. Ecol. Res.*, 28, 57–92.

Goetz, S.J., Bunn, A.G., Fiske, G.J. & Houghton, R.A. (2005). Satellite-observed photosynthetic trends across boreal North America associated with climate and fire disturbance. *Proc. Natl. Acad. Sci. USA*, 102, 13521–13525.

Goetz, S.J., Fiske, G.J. & Bunn, A.G. (2006). Using satellite time-series data sets to analyze fire disturbance and forest recovery across Canada. *Remote Sens. Environ.*, 101, 352–365.

Gonzalez, P., Neilson, R.P., Lenihan, J.M. & Drapek, R.J. (2010). Global patterns in the vulnerability of ecosystems to vegetation shifts due to climate change. *Global Ecol. Biogeogr.*, 19, 755–768.

Hansen, M.C., DeFries, R.S., Townshend, J.R.G., Carroll, M., Dimiceli, C. & Sohlberg, R.A. (2003). Global percent tree cover at a spatial resolution of 500 meters: first results of the MODIS vegetation continuous fields algorithm. *Earth Interact.*, 7, 1–15.

Hickling, R., Roy, D.B., Hill, J.K., Fox, R. & Thomas, C.D. (2006). The distributions of a wide range of taxonomic groups are expanding polewards. *Glob. Change Biol.*, 12, 450–455.

Hinzman, L., Bettez, N., Bolton, W., Chapin, F., Dyurgerov, M., Fastie, C. *et al.* (2005). Evidence and implications of recent climate change in northern Alaska and other arctic regions. *Clim. Change*, 72, 251–298.

Hogberg, P., Fan, H.B., Quist, M., Binkley, D. & Tamm, C.O. (2006). Tree growth and soil acidification in response to 30 years of experimental nitrogen loading on boreal forest. *Glob. Change Biol.*, 12, 489–499.

Hogg, E.H., Brandt, J.P. & Michaelian, M. (2008). Impact of regional drought on the productivity, dieback and biomass of western Canadian aspen forests. *Can. J. For. Res.*, 38, 1373–1384.

Hollander, M. & Wolfe, D.A. (1973). *Nonparametric Statistical Methods*. John Wiley & Sons, New York.

IPCC (2007). *Climate Change 2007: The Physical Science Basis. Contribution of Working Group I to the Fourth Assessment Report of the Intergovernmental Panel on Climate Change*. Cambridge University Press, Cambridge.

Jones, J.B.J., Petrone, K.C., Finlay, J.C., Hinzman, L.D. & Bolton, W.R. (2005). Nitrogen loss from watersheds of interior Alaska underlain with discontinuous permafrost. *Geophys. Res. Lett.*, 32, L02501.

Juday, G.P., Barber, V., Vaganov, E., Rupp, S., Sparrow, S., Yarie, J. *et al.* (2005). Forests, land management, and agriculture. In: *Arctic Climate Impact Assessment* (eds Symon, C., Arris, L. & Heal, B.). Cambridge University Press, Cambridge, pp. 781–862.

Kaufmann, R.K., D'Arrigo, R.D., Laskowski, C., Myneni, R.B., Zhou, L. & Davi, N.K. (2004). The effect of growing season and summer greenness on northern forests. *Geophys. Res. Lett.*, 31, L09205.

Kimball, J.S., Zhao, M., McGuire, A.D., Heinsch, F.A., Clein, J., Calef, M. *et al.* (2007). Recent climate-driven increases in vegetation productivity for the western Arctic: evidence of an acceleration of the northern terrestrial carbon cycle. *Earth Interact.*, 11, 0004.

Lloyd, A.H., Rupp, T.S., Fastie, C.L. & Starfield, A.M. (2002). Patterns and dynamics of treeline advance on the Seward Peninsula, Alaska. *J. Geophys. Res.-Atm.*, 107, 8161, 15 pp.

Lucht, W., Prentice, I., Myneni, R., Sitch, S., Friedlingstein, P., Cramer, W. *et al.* (2002). Climatic control of the high-latitude vegetation greening trend and Pinatubo effect. *Science*, 296, 1687–1689.

Lucht, W., Schaphoff, S., Erbrecht, T., Heyder, U. & Cramer, W. (2006). Terrestrial vegetation redistribution and carbon balance under climate change. *Carbon Balance Manage.*, 1, 6, 7 pp.

Malmström, C.M. & Raffa, K.F. (2000). Biotic disturbance agents in the boreal forest: considerations for vegetation change models. *Glob. Change Biol.*, 6, 35–48.

McGuire, A.D., Anderson, L.G., Christensen, T.R., Dallimore, S., Guo, L., Hayes, D.J. *et al.* (2009). Sensitivity of the carbon cycle in the Arctic to climate change. *Ecol. Monogr.*, 79, 523–555.

McGuire, A.D., Ruess, R.W., Lloyd, A., Yarie, J., Clein, J.S. & Juday, G.P. (2010). Vulnerability of white spruce tree growth in interior Alaska in response to climate variability: dendrochronological, demographic, and experimental perspectives. *Can. J. For. Res.*, 40, 1197–1209.

McKenney, D.W., Pedlar, J.H., Papadopol, P. & Hutchinson, M.F. (2006). The development of 1901–2000 historical monthly climate models for Canada and the United States. *Agr. Forest Meteorol.*, 138, 69–81.

Myneni, R.B., Hall, F.G., Sellers, P.J. & Marshak, A.L. (1995). The interpretation of spectral vegetation indices. *IEEE Trans. Geosci. Remote Sens.*, 33, 481–486.

Myneni, R.B., Keeling, C.D., Tucker, C.J., Asrar, G. & Nemani, R.R. (1997). Increased plant growth in the northern high latitudes from 1981–1991. *Nature*, 386, 698–702.

Peñuelas, J. & Boada, M. (2003). A global change-induced biome shift in the Montseny mountains (NE Spain). *Glob. Change Biol.*, 9, 131–140.

Rahmstorf, S., Cazenave, A., Church, J.A., Hansen, J.E., Keeling, R.F., Parker, D.E. *et al.* (2007). Recent climate observations compared to projections. *Science*, 316, 709.

Scholze, M., Knorr, W., Arnell, N.W. & Prentice, I.C. (2006). A climate-change risk analysis for world ecosystems. *Proc. Natl. Acad. Sci. USA*, 103, 13116–13120.

Sitch, S., Cox, P.M., Collins, W.J. & Huntingford, C. (2007). Indirect radiative forcing of climate change through ozone effects on the land-carbon sink. *Nature*, 448, 791–794.

Tape, K., Sturm, M. & Racine, C. (2006). The evidence for shrub expansion in Northern Alaska and the Pan-Arctic. *Glob. Change Biol.*, 12, 686–702.

Tarnocai, C., Canadell, J.G., Schuur, E.A.G., Kuhry, P., Mazhitova, G. & Zimov, S. (2009). Soil organic carbon pools in the northern circumpolar permafrost region. *Global Biogeochem. Cycles*, 23, GB2023.

Tucker, C.J., Pinzon, J., Brown, M., Slayback, D., Pak, E., Mahoney, R. *et al.* (2005). Extended AVHRR 8-km NDVI data set compatible with MODIS and SPOT vegetation NDVI data. *Int. J. Remote Sens.*, 26, 4485–4498.

Verbyla, D. (2008). The greening and browning of Alaska based on 1982–2003 satellite data. *Global Ecol. Biogeogr.*, 17, 547–555.

Viereck, L.A., Dyrness, C.T. & Foote, M.J. (1993). An overview of vegetation and soils of the floodplain ecosystem of the Tanana River, interior Alaska. *Can. J. For. Res.*, 23, 889–898.

Vingarzan, R. (2004). A review of surface ozone background levels and trends. *Atmos. Environ.*, 38, 3431–3442.

Vogelsang, T.J. (1998). Trend function hypothesis testing in the presence of serial correlation. *Econometrica*, 66, 123–148.

Way, D.A. & Oren, R. (2010). Differential responses to changes in growth temperature between trees from different functional groups and biomes: a review and synthesis of data. *Tree Physiol.*, 30, 669–688.

Wittig, V.E., Ainsworth, E.A., Naidu, S.L., Karnosky, D.F. & Long, S.P. (2009). Quantifying the impact of current and future tropospheric ozone on tree biomass, growth, physiology and biochemistry: a quantitative meta-analysis. *Glob. Change Biol.*, 15, 396–424.

Yarie, J. (2008). Effects of moisture limitation on tree growth in upland and floodplain forest ecosystems in interior Alaska. *For. Ecol. Manage.*, 256, 1055–1063.

Zhang, X., Friedl, M.A. & Schaaf, C.B. (2006). Global vegetation phenology from Moderate Resolution Imaging Spectroradiometer (MODIS): evaluation of global patterns and comparison with *in situ* measurements. *J. Geophys. Res.*, 111, G04017.

Zhang, K., Kimball, J.S., Hogg, E.H., Zhao, M., Oechel, W., Cassano, J.J. *et al.* (2008). Satellite-based model detection of recent climate-drive changes in northern high-latitude vegetation productivity. *J. Geophys. Res.*, 113, G03033, 13 pp.

Zhao, M. & Running, S.W. (2010). Drought-induced reduction in global terrestrial net primary production from 2000 to 2009. *Science*, 329, 940–943.

Zhou, L., Tucker, C.J., Kaufmann, R.K., Slayback, D., Shabanove, N.V. & Myneni, R.B. (2001). Variations in northern vegetation activity inferred from satellite data of vegetation index during 1981 and 1999. *J. Geophys. Res.*, 106, 20069–20083.

SUPPORTING INFORMATION

Additional Supporting Information may be found in the online version of this article:

Appendix S1 Background on the use of stable carbon isotopes in wood as indicators of drought conditions.

Figure S1 Map of growing season length in Alaska derived from Moderate Resolution Imaging Spectroradiometer (MODIS) data.

Figure S2 Theoretical example of gross productivity (Prs) calculation from yearly NDVI time series.

Figure S3 Absolute difference in trends in radial growth and remotely sensed gross productivity ($|\tau RG - \tau Prs|$) as a function of tree-ring sample size and area burned.

Figure S4 Time series of mean tree-ring widths and growing season NDVI for individual stands.

Figure S5 Daily tropospheric ozone measurements at Denali National Park since 1998.

Figure S6 Correlation between mean tree-ring width and monthly temperature.

Figure S7 Summer temperature and vapour pressure deficit from 1988 to 2008 at the Bonanza Creek Long Term Ecological Research site.

Figure S8 (a) Comparison of linear trends in Prs over the periods 1982–1991 and 1994–2008, and (b) the linear trend in Prs over the period 2000–2008.

Table S1 Overview of tree-ring sampling sites and observed trends in Prs.

As a service to our authors and readers, this journal provides supporting information supplied by the authors. Such materials are peer-reviewed and may be re-organized for online delivery, but are not copy edited or typeset. Technical support issues arising from supporting information (other than missing files) should be addressed to the authors.

Editor, Josep Penuelas
Manuscript received 20 September 2010
First decision made 27 October 2010
Second decision made 6 January 2011
Manuscript accepted 26 January 2011